INTERNATIONAL JOURNAL OF SUSTAINABLE CONSTRUCTION ENGINEERING AND TECHNOLOGY
VOL.14 NO. 4 (2023) 79-93

IJSCET

http://publisher.uthm.edu.my/ojs/index.php/ijscet

ISSN : 2180-3242 e-ISSN : 2600-7959

International Journal of Sustainable Construction Engineering and Technology

An Investigation of the Performance of the ANN Method for Predicting the Base Shear and Overturning Moment Time-Series Datasets of an Offshore Jacket Structure

Ramin Vafaei Poursorkhabi[1, 2*], Amin Hosseinchi Gharehaghaji[3], Alireza Naseri[1, 2]

[1]Department of Civil Engineering, Tabriz Branch,
Islamic Azad University, Tabriz, IRAN

[2]Robotics & Soft Technologies Research Centre, Tabriz Branch,
Islamic Azad University, Tabriz, IRAN

[3]Department of Geomatics Engineering, Faculty of Civil Engineering,
University of Tabriz, Tabriz, IRAN

*Corresponding Author

DOI: https://doi.org/10.30880/ijscet.2023.14.04.007
Received 23 December 2022; Accepted 17 October 2023; Available online 17 October 2023

Abstract: The primary purpose of the current study was to investigate the performance of artificial neural networks to predict the time series of the water surface level (WSL), base shear, and overturning moment using two types of ANN models: Nonlinear Autoregressive models with exogenous inputs (NARX) and Nonlinear Autoregressive models (NAR). After determining the suitable model, NARX, the possibility of predicting the time series of the base shear and the overturning moment data was investigated by considering the water surface level and time as the multivariable model inputs. A jacket model with a height of 4.55m was fabricated and tested in the 402m-long wave flume of the NIMALA marine laboratory. The jacket was tested at the water depth of 4m and subjected to random waves with a JONSWAP energy spectrum. Three input wave heights were chosen for the tests: 20cm, 23cm, and 28cm. The findings showed that using the NARX neural network is a convenient method to predict the base shear and overturning moment values based on the water surface level data as input values. Finally, after suitable neural network determination, using the NARX neural network, the correlation value (R) for calculating water surface level (WSL), Base Shear, and Overturning Moment were obtained as 0.994, 0.97, and 0.94, respectively.

Keywords: Jacket structure, base shear, overturning moment, random waves, Nonlinear Autoregressive Models with Exogenous Inputs (NARX), Artificial Neural Network (ANN)

1. Introduction

The jacket-type platform is the most common offshore structure constructed for extracting oil and gas from reservoirs below the seabed (Osgouei et al., 2021). It is a bottom-fixed offshore structure with many advantages (Guo et al., 2018). It consists of three main parts: a superstructure or topside, a substructure or jacket, and the foundation or piles. The jacket substructure is a steel space frame fabricated by welding the thin-walled circular hollow section (CHS) members called tubular (Osgouei et al., 2021).

*Corresponding author: raminvafaei@yahoo.com

The jacket platform is primarily subjected to random wave excitations that have the characteristics of both short-term random fluctuations and long-term random evolvement (Li & Huang, 2020). Due to the presence of random waves, it is crucial to study the behaviour of the structure against these random waves (Vafaeipour et al., 2022). The calculation of forces exerted on tubular structures (e.g., jacket substructures) due to random sea waves has a long extensive history and includes the tubular investigated in experimental, numerical, and theoretical studies (Osgouei et al., 2021). One of these methods, which is powerful and the most typical method applied to modelling and predicting the behaviour of systems, is the Artificial Neural Network (ANN). The ANN is a set of algorithms used in machine learning for modelling the data (Mousavi et al., 2021). Neural networks emulate the human brain and gain knowledge through learning (Afroz et al., 2018). Over the past few years, artificial neural network models have been developed for various fields, including time series prediction. Several types of ANNs, like the Nonlinear Autoregressive Exogenous Neural Network (NARX), Nonlinear Autoregressive Neural Network (NAR), and Recurrent Neural Network (RNN), are used for the prediction of time series (Sarkar et al., 2019).

Several studies have been conducted on the effects of wave forces on slender bodies for various loading cases. One of the most famous studies on the applications of wave forces to cylindrical piles was conducted by Morison et al. (1950), in which the in-line wave force was assumed to be the linear sum of two components: drag force and inertia force (Morison et al., 1950). Chan et al. (1995) studied the effects of plunging waves on vertical cylinders (Chan et al., 1995). Vafaeipour et al. (2019) studied the experimental investigation of the interaction between vertical flexible seawalls and random sea waves. The impulsive breaking wave forces on piles were investigated by Goda et al. (Goda et al., 1966). Murgoitio et al. (2020) studied the impact forces of nearly-breaking waves on vertical circular cylinders (Esandi et al., 2020). An experimental study investigated the stability of coastal structures and breakwaters against the force of sea waves with different heights and periods (Alami et al., 2022). Hildebrant (2013) investigated the hydrodynamic effects of breaking waves on offshore wind turbine structures (Hildebrandt, 2013). Sruthi and Sriram (2017) studied the impacts of wave loads on jacket structures in an intermediate water depth (Sruthi & Sriram, 2017). Naseri et al. (2022) studied the impact wave forces on the reinforced rubble mound breakwater and measured the deformation of the structure.

Numerous studies have also addressed the applications of neural networks and time-series predictions. Nguyen and Dou (2019) investigated the application of a hybrid model of artificial neural network–particle swarm optimization (ANN-PSO) in predicting the behaviour of channel connectors embedded in normal and high-strength concrete (HSC) (Shariati et al., 2019). Ettefagh (2020) developed an effective deep neural network for extracting the damage-sensitive features from the frequency data of vibration signals to detect the damage to mechanical systems in the presence of uncertainties such as modelling errors, measurement errors, and environmental noises (Mousavi et al., 2021). Jiang (2018) presented a damage identification method for offshore jacket platforms using partially-measured modal results from artificial intelligence neural networks (Guo et al., 2018). Haddara (2010) discussed damage detection in offshore jacket platforms subjected to random loads using a hybrid method of random decrement signature and neural networks (Shariati et al., 2019). Camelo (2018) showed two innovative hybrid methodologies capable of performing short- and long-term wind speed predictions from the mathematical junction of two classical time series models: the Autoregressive Integrated Moving Average with Explanatory Variable (ARIMAX) and the Holt-Winters (HW); both models were combined with Artificial Neural Networks (ANN) (do Nascimento Camelo et al., 2018). Shariati (2020) investigated the application of artificial intelligence (AI) techniques like artificial neural networks (ANN) - as sub-branches of the SC methods - in the behaviour prediction of an innovative type of C-shaped shear connector called Tilted Angle Connector (Shariati et al., 2020). Kermani (2019) conducted a survey on the feasibility of utilizing soft computing models in predicting emission factors (gaseous H2S) based on five input parameters, including the total dissolved sulfides and biochemical oxygen demand (BOD5), temperature, flow rate, and PH. Thus, multivariate nonlinear autoregressive exogenous (NARX) neural networks were developed and applied to predict weekly H2S in four WWTPS (Zounemat-Kermani et al., 2019). The base shear and overturning moment are crucial parameters for analysing and designing offshore jacket structures subjected to random wave loading (Osgouei et al., 2021).

In this research, we have tried to predict the time series related to water surface level (WSL), base shear, and overturning moment by using a neural network and evaluating the neural network performance in this case. In addition, we have tried to assess the possibility of estimating base shear and overturning moment values using the estimated WSL values using a suitable neural network.

2. Data

2.1 The Wave-Maker Flume

The experiments of the present research were conducted in the NIMALA marine laboratory. Its wave flume, the biggest one in Iran, is 402m long, 6m wide, and 4.5m high (Fig. 1). The water depth in the flume was 4m. NIMALA lab has received ISO/IEC 17095 2005 and ISO 9001:2015 certificates (NIMALA, 2018). The equipment installation, setup, and calibration were accomplished according to the ITTC documents (ITTC, 2008).

The piston-type wave-maker paddle can generate regular and random waves with the frequency content of Bretschneider, Pierson-Moskowitz (P-M), and JONSWAP wave spectra. The maximum wave height that the wave-

maker can achieve is 50cm. Wave probes of the resistance sensor type are connected to a data-logging system through an amplifier. They are cable of recording the time series of the water surface level with high accuracy. The wave flume has a 7.6mX7.0m manned chariot with a speed range of 0.5–10 m/s. Reticulated panels fabricated the wave absorber at the end of the flume to minimize the wave reflection and to avoid interference between the incident and reflected waves. However, since the flume was quite long and the duration of each experiment was relatively short, data recording was performed before the waves reached the flume end; consequently, wave reflection was generally not an issue.

Fig. 1 - The wave flume and manned chariot of NIMALA marine laboratory

2.2 Models of the Jacket Structure

The jacket structure investigated in the present study was a scaled model of a C13 jacket installed in the South Pars gas field of the Persian Gulf. The height of the actual jacket is 80m operating at a water depth of 72m. With a scale factor of 1 to 18, the jacket model was 4.4m high and installed in the flume at a water depth of 4m. The distance between the jacket and the wave maker was 70m, while its distance from the flume end was 332m. Fig. 2 shows an isometric view of the jacket structure.

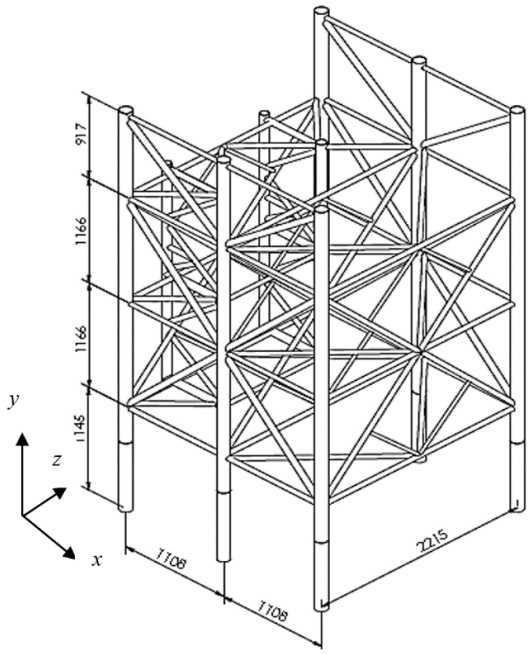

Fig. 2 - An isometric view of the jacket model (mm)

Fig. 3 illustrates the longitudinal section of the wave flume, the jacket structure, and the equipment. Fig. 4 shows the dry jacket structure (Fig. 4a) and the jacket installed in the flume without the wave barrier (Fig. 4b).

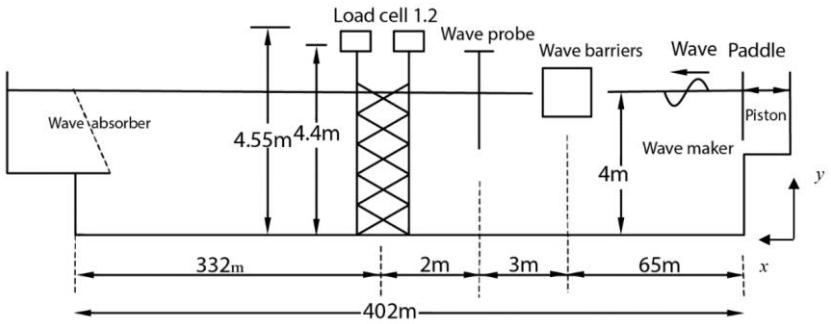

Fig. 3 - Longitudinal section of the wave flume along with the jacket, wave barrier, and the equipment

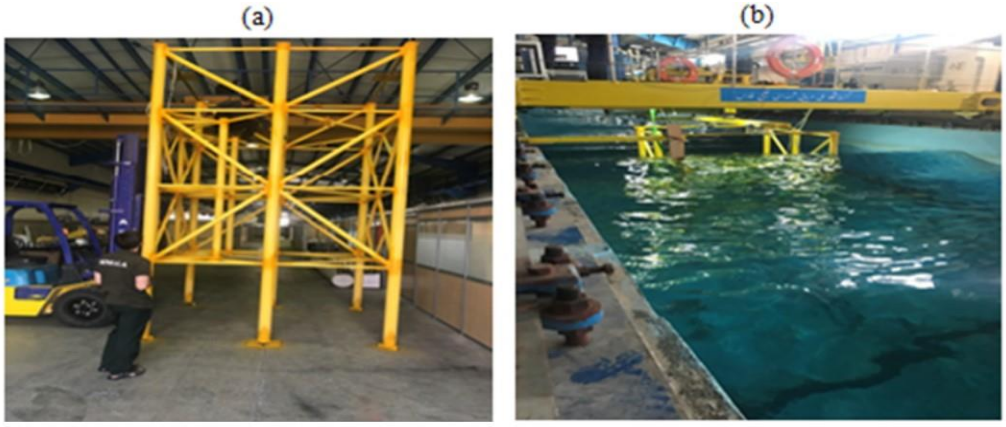

Fig. 4 - (a) Dry jacket structure; (b) the jacket installed in the flume without the wave barrier

2.3 Data Recording and Interpretation

Three sets of recordings were performed in the data recording phase to determine the jacket structure's water surface level, base shear, and overturning moment. The water surface level was measured using resistance-type wave probes, and the still water level (SWL) was set as the datum. The wave probes were installed between the jacket and the wave-maker at 2m from the jacket. The time step between the recorded data was 0.05s. Hence, 8000 levels were recorded during a 400s experiment. The recording of the force data was also performed with 0.05s time steps considering the accurate calibration of the wave probes and the load cells. Load cells that were the product of Wonbang Forcetech had a force measurement capacity of 400N and 50N in the longitudinal and lateral directions, respectively (Fig. 5).

Fig. 5 - Load cells used in the present research to measure the wave forces

Since the exerted force during an extreme wave was predicted to be larger than the capacity of a single load cell, two load cells were used to make sure that the total wave force would be recorded accordingly. The correlation between the two load cells was crucial. Hence, they were calibrated so there was no phase lag between their records. The load cells were installed at the top of the structure instead of its bottom to ease access and control during successive experiments (Fig. 6a). Obviously, the base shear of the jacket structure would be equal to the total force recorded by the load cells (Fig. 6b). The overturning moment can be calculated as FLC, where FLC is the total wave force recorded by the load cells Assuming pin support at the bottom of the jacket model; moreover, h is the jacket height (4.4m) plus the height of the load cell position relative to the jacket top (0.15m), i.e., h = 4.55m (Fig. 6c).

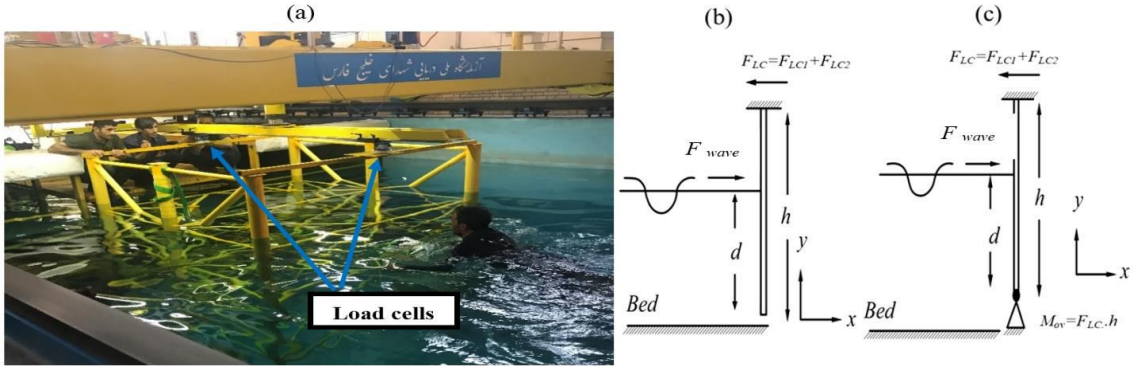

Fig. 6 - (a) Installation of load cells; (b) Base shear (FBS) recording mechanism; (c) Overturning moment (M_{ov}) recording mechanism

For example, Fig. 7 shows a sample time-series set of water surface level, base shear, and overturning moment. The generated waves had the frequency content of the JONSWAP energy spectrum with $\gamma = 3.3$. As mentioned, the water depth was 4m, and the data recording frequency was 20 Hz. The details of all experiments conducted during the present research are given in Table 1.

Table 1 - Details of all experiments conducted during the present research

Base shear recording tests				
Jacket (without the wave barrier)	Wave-maker input wave height (cm)	20	23	28
	Wave condition	Nonbreaking	Nonbreaking	Nonbreaking
	Test ID	FN20	FN23	FN28
Overturning moment recording tests				
Jacket (without the wave barrier)	Wave-maker input wave height (cm)	20	23	28
	Wave condition	Nonbreaking	Nonbreaking	Nonbreaking
	Test ID	MN20	MN23	MN28

In the case of the jacket without a wave barrier, four values were designated for the input wave height of the wave-maker (Hw-in): 20, 23, 28, and 30cm.

For H = 30cm, the waves were broken; on the other hand, nonbreaking wave conditions prevailed for the wave height values. The present study was focused only on the latter case. The input value of the wave period defined for the wave-maker was 1.8s during the experiments.

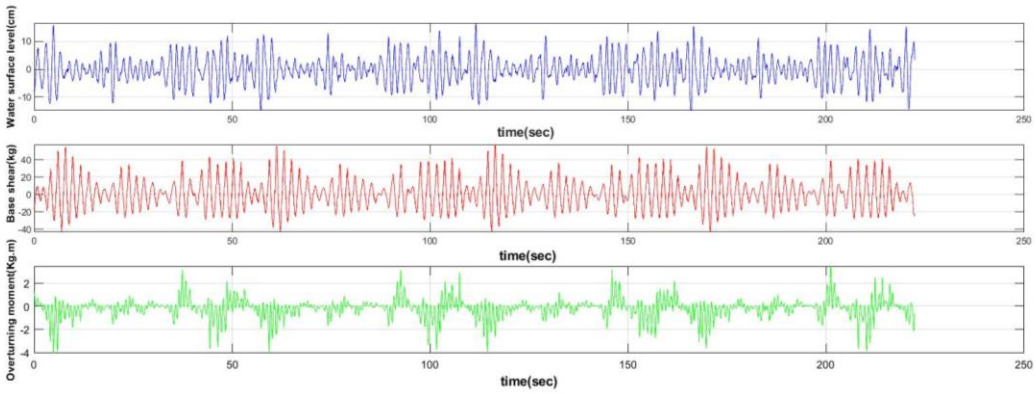

Fig. 7 - Sample time series of recorded data

3. Methodology

Artificial Neural Networks (ANNs) are used for many applications like clustering, recognition, pattern classification, optimization, function approximation, and prediction (Boussaada et al., 2018). In the field of prediction, the neural network model has been widely used in predicting chaotic time series (Xiu & Zhang, 2017). ANNs are designed based on biological neural systems and mathematical relationships; therefore, they have a powerful potential to learn, store, and recall information most of the time.

A neural network can be classified into static and dynamic (Shahrisvand et al., 2014). In dynamic networks, input values include not only current inputs but also current or previous output values. Predicting chaotic time series with neural networks is a traditional practical problem of dynamic systems (Diaconescu, 2008). Two applicable standard models are involved in predicting the time series: Nonlinear Autoregressive models with exogenous inputs (NARX models) and Nonlinear Autoregressive (NAR models). A Nonlinear Autoregressive (NAR) network is a dynamic neural network that is convenient for predicting time series where only one set of series is involved.

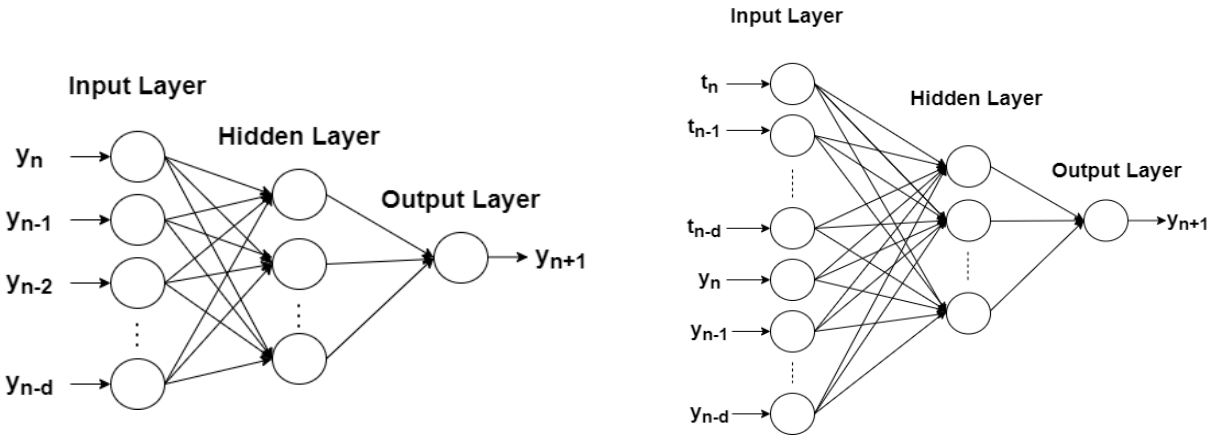

Fig. 8 - (a) Structure of the NAR neural network, (b) Structure of the NARX neural network

The future values of a time series y(t) are predicted only based on the past values of that series (Wei et al., 2012):

$$y(t) = f\ (y(t-1), y(t-2)..., y(t-d)) \quad (1)$$

Equation (1) shows how the NAR model is used to predict the value of a data series at the time t, y(t) using d past values of the time series (Blanchard & Samanta, 2020). In other words, the NAR model extracted generic principles from the past values of the time series to predict its future values (Taherdangkoo et al., 2020).

The Nonlinear Autoregressive model with exogenous inputs (NARX model) is a powerful class of dynamic neural networks, and it has been proven that it is well suited for nonlinear modelling systems (especially time series) (Shahrisvand et al., 2014). The NARX prediction is based on the last output values with exogenous input for the estimation of future ones (Sarkar et al., 2019):

$$y(t) = f\ (y(t-1), y(t-2)..., y(t-d), x(t-1), x(t-2)..., x(t-d)) \quad (2)$$

In the NARX model, future values of a time series y(t) are predicted from past values of y(t) and another external series x (t). Therefore, compared to the Nonlinear Autoregressive (NAR) model, NARX can consider external (exogenous) input for predicting the time series y(t) and detecting changes in model parameters due to external conditions, as seen in equation (2), where x(t) is the observation of the exogenous input at time t (Raptodimos & Lazakis, 2020). The d features are called feedback delays, shown as 1:2 in Fig.12 and Fig.13. The number of feedback delays and neurons per hidden layer is optimized through trial-and-error testing to obtain the network architecture for the best performance (Blanchard & Samanta, 2020). Fig.8a shows the structure of the NAR neural network model with just a single hidden layer (Fig8a), and Fig.8b shows the NARX neural network model with just a single hidden layer, too (Fig.8b).

Traditionally, topology identification has been based on trial and error, heuristics sometimes followed by trial and error, and pruning or constructive methods, as discussed in the following section. None of these methods has the theoretical rigor of revealing optimal or at least near-optimal solutions (Stathakis, 2009). The number of hidden layers and neurons in the hidden layer are 1 and 10, respectively (by MATLAB software defaults). The activation function used in the input and hidden layer neurons is sigmoid. This function is especially advantageous in neural networks trained by back-propagation algorithms (Levenberg-Marquardt algorithm). Furthermore, the sigmoid function presents the advantage of being derivable, which makes the weight learning of the neural network easier. In most neural studies, the output layer's activation functions are linear (Boussaada et al., 2018).

A time series is an array of vectors that depends on time. Since the current study dealt with time-series data, the ANN technique was implemented for predicting the time series of water surface level, base shear, and overturning moment. In the first phase, the performance of NAR and NARX models was evaluated in terms of predicting the time series of water surface level. After analysing the results and as the goal was to introduce the predicted WSL data as the

input of a multivariable NARX neural network, the suitable model capable of precisely predicting the WSL time series was selected. In the next phase, the assumption concerning whether it was possible or not to predict the base shear and overturning moment time series based on the time and water surface level data was evaluated.

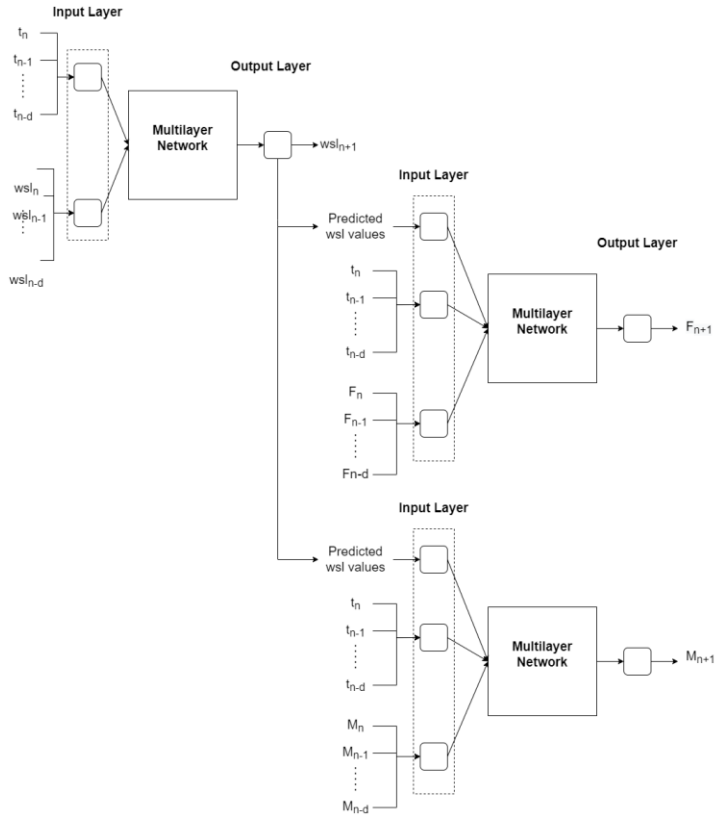

Fig. 9 - Progress of prediction issue

Considering the descriptions, Fig.9 shows the progress of predicting WSL, base shear, and overturning moment using the suitable ANN model (Fig.9). In this study, the number of data used for WSL, base shear, and the overturning moment is 4448 in the time range 0-222.35s with 0.05 seconds step.

The ANN calculations were performed in MATLAB, and the data were divided into the training (70%), evaluation (15%), and test (15%) data. The Levenberg-Marquardt (LM) algorithm was used in the case of the training network. The algorithm was used to estimate the parameters of the neural network as it could lead to faster convergence within a few cycles following a significant disturbance (Arif et al., 2009). The Levenberg-Marquardt algorithm (LMA) can be used to solve nonlinear least-squares problems. This method minimizes the sum of squared residuals; residuals mean the difference between the actual values and the values obtained by the function. LMA updates the function parameter between the Gauss-Newton and gradient descent methods for updating. This iterative calculation method locates a local minimum of a multivariate function, expressed as the sum of squares of various nonlinear, real-valued functions (Amin et al., 2015). It should be noted that this algorithm typically requires more memory but takes less time.

It should be noted that the network was created and trained in an open-loop method which is more efficient than closed-loop training. Open-loop allows supplying the network with correct past outputs and training it to produce current outputs.

4. Results and Discussion

According to what was discussed, first, the NAR and NARX neural networks were applied to predict the WSL time series. Fig.10 shows the correlation values for the NAR neural network (Fig.10). Fig. 11 shows the correlation values for the NARX neural network (Fig.11). These two images show the correlation values for training, evaluation, test stages, and all the data. The correlation value obtained for estimating all the WSL data with the NAR model is about 0.028; with the NARX model, about 0.994 has been achieved.

Given the correlation values (R) obtained, it was found that the NAR neural network was not well-trained and could not be used to predict the WSL values. Then, the NARX neural network model was executed for the WSL time series prediction. As shown in Fig.9, the predicted WSL time series and time data were applied as the inputs of base shear and overturning moment multivariable NARX models.

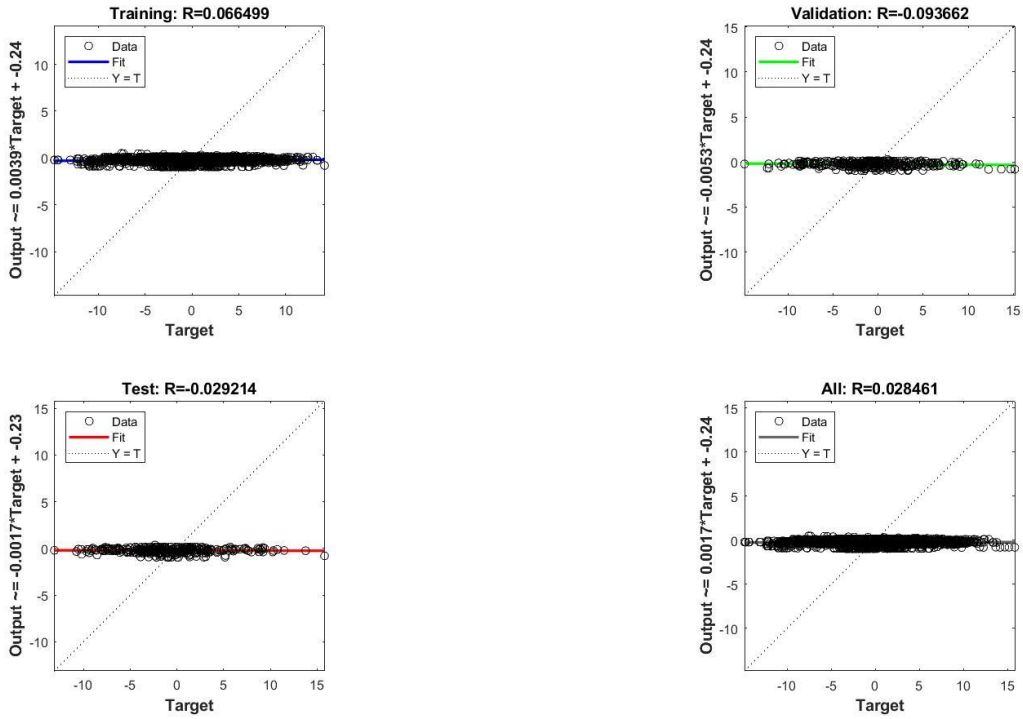

Fig. 10 - Correlation values (R) for predicted WSL time series using NAR model

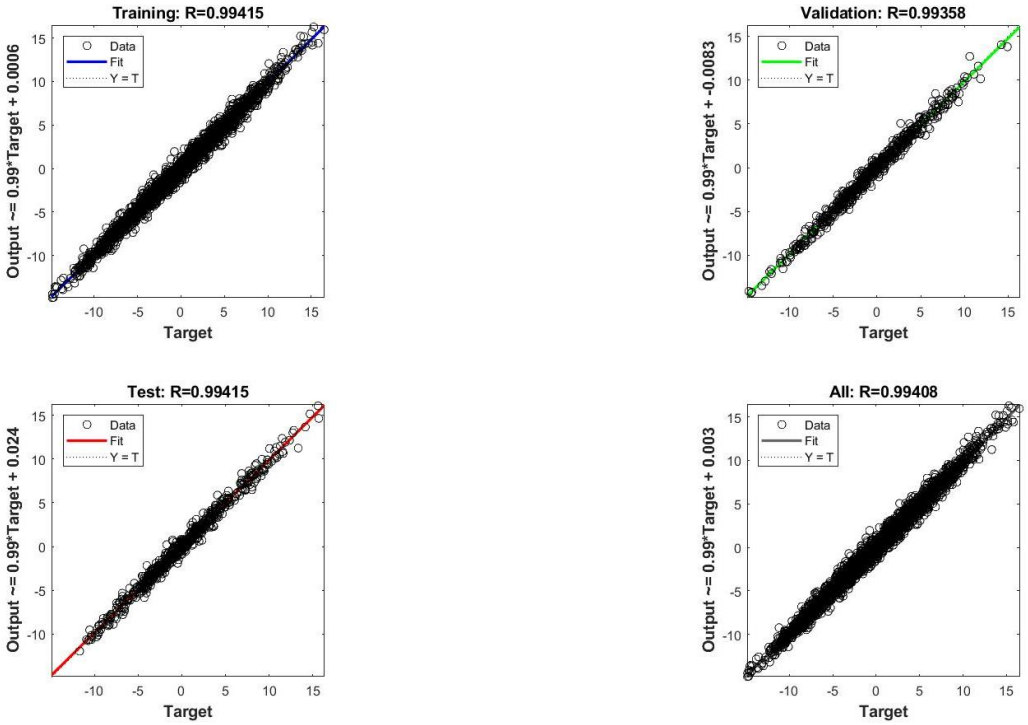

Fig. 11 - Correlation values (R) for predicted WSL time series using NAR model

Fig.12 shows the NARX model structure for WSL calculation, and Fig.13 shows the NARX model structure for Base Shear and Overturning Moment calculation. x(t), y(t) in Fig.12 and x(t, WSL) and y(t) in Fig.13 represent the inputs of the network. The size of the input vectors for x(t) and y(t) equals r1*1 and r^2*1, respectively. The size of the input vector x(t, WSL) is equal to r^1*1, too. In the first layer (hidden layer), $IW_1^{1,1}$ represents the input weights for x(t)

and x(t, WSL), and $IW_2^{1,1}$ represents the input weights for y(t), whose size is respectively done. It is equal to $s^1 * r^1$ and $s^1 * r^2$, where s^1 represents the number of hidden layer neurons. $LW^{2,1}$ represents the layer weights with size $s^2 * s^1$, whose s^2 represents the number of neurons in the output layer. Vector b^1 and vector b^2 represent the bias of the hidden layer with size s^1*1 and the bias of the output layer with size 1*1, respectively. F^1 represents the sigmoid activation function for the hidden layer, and f^2 represents the linear activation function for the output layer. g(t) represents the estimated value for WSL, and g(t, WSL) represents the estimated value for Overturning Moment and Base Shear.

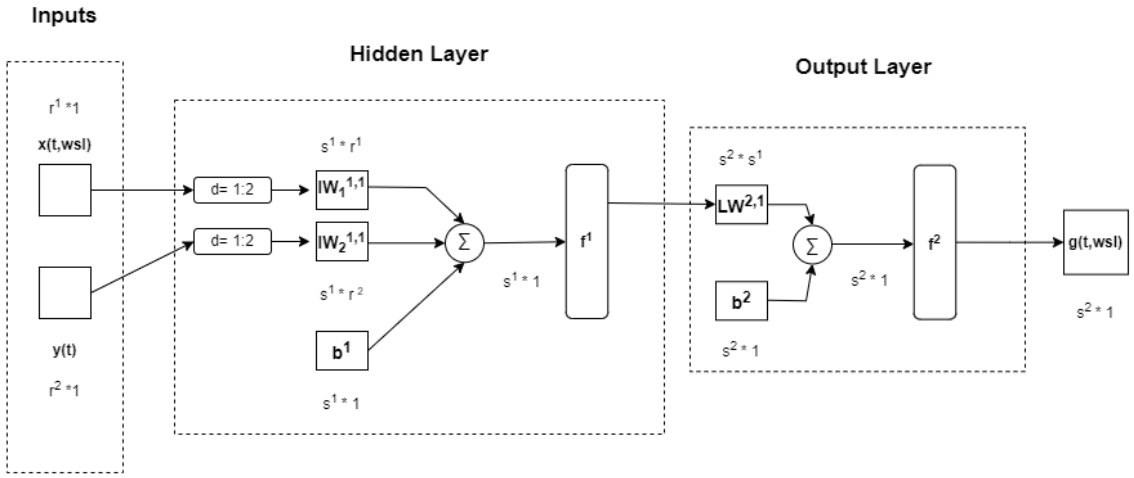

Fig. 12 - NARX model structure for estimating WSL data

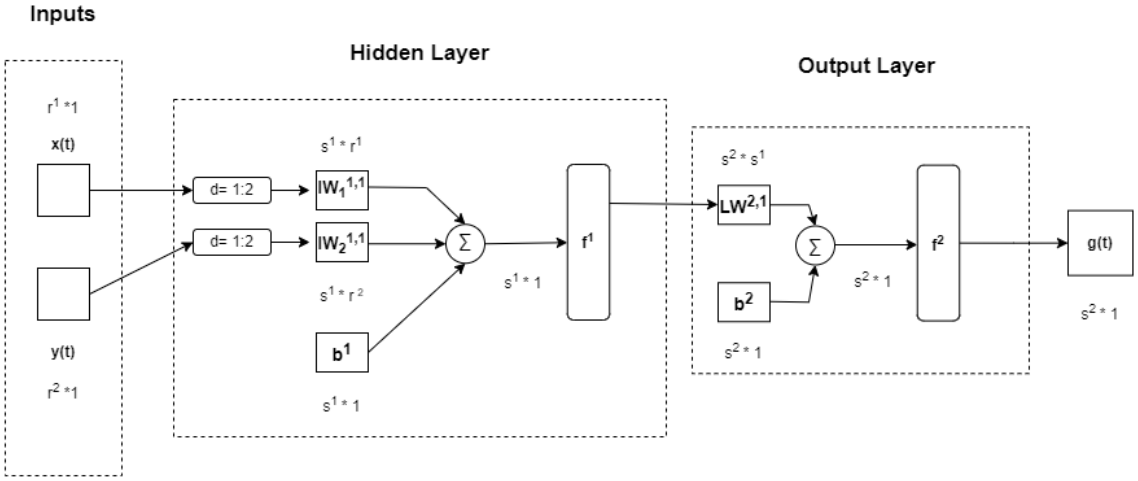

Fig. 13 - NARX model structure for estimating base shear and overturning moment data

Fig.14 and Fig.15 show the correlation values for the NARX neural network performed for predicting the base shear and overturning moment time series, respectively (Fig.14 - Fig.15). The correlation values obtained for estimating the entire base shear and overturning moment data with the NARX model is about 0.97 and 0.944 respectively.

The mathematical relation between the activation functions, inputs, weights, and biases for calculating WSL is shown in Equation 3, and the Base Shear and Overturning Moment are shown in Equation 4.

$$g(t) = f^{2}\left\{LW^{2,1}\left\{f^{1}\left[(IW_1^{1,1} * x(t) + (IW_2^{1,1} * y(t)) + b^{1}\right]\right\} + b^{2}\right\} \quad (3)$$

$$g(t,wsl) = f^{2}\left\{LW^{2,1}\left\{f^{1}\left[(IW_1^{1,1} * x(t,wsl) + (IW_2^{1,1} * y(t)) + b^{1}\right]\right\} + b^{2}\right\} \quad (4)$$

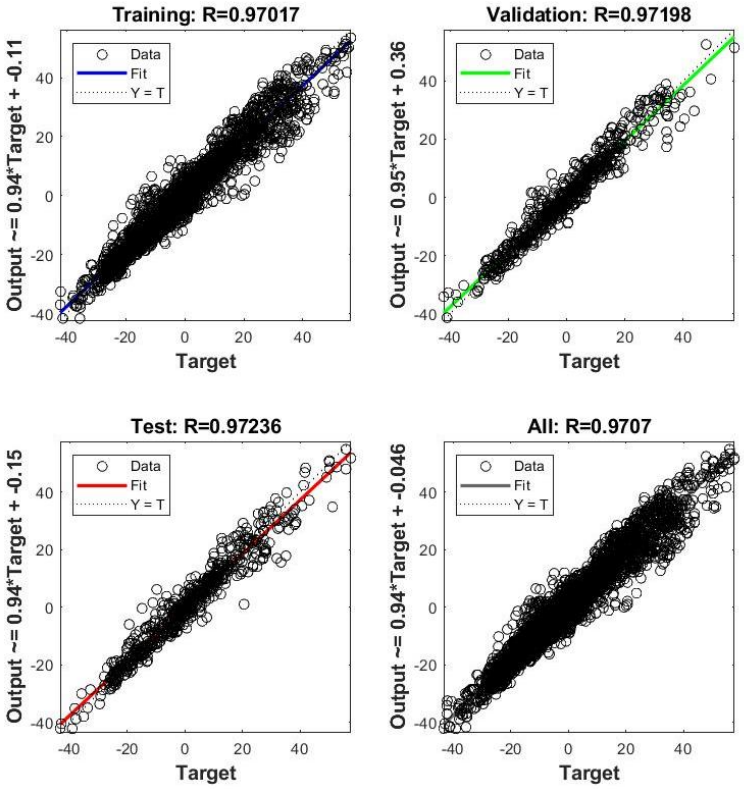

Fig. 14 - Correlation values (R) for the predicted base shear time series using NARX model

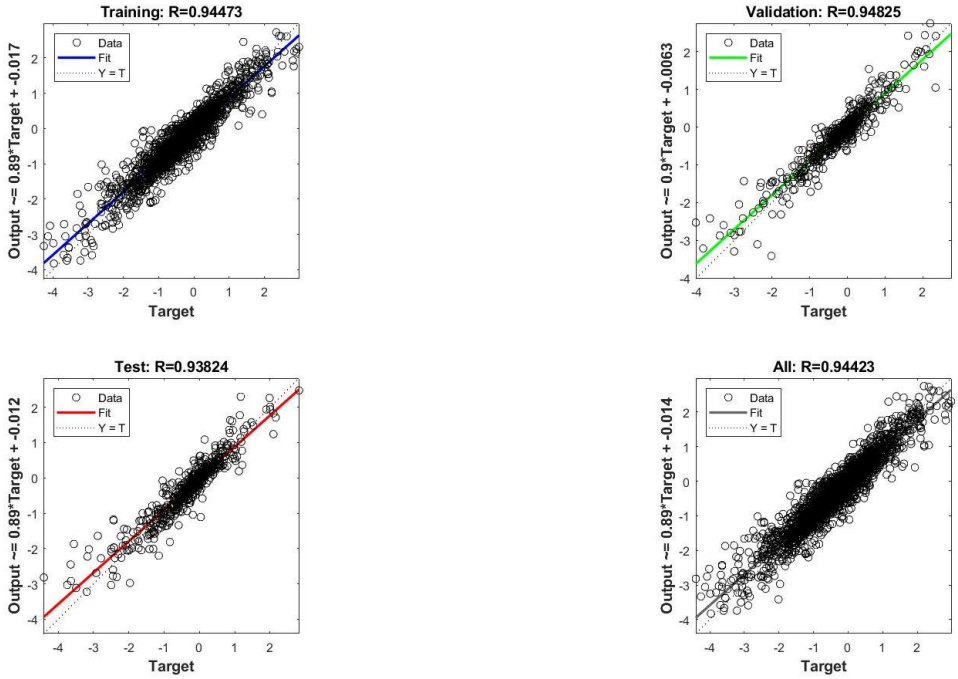

Fig. 15 - Correlation values (R) for the predicted overturning moment time series using NARX model

The optimum values of weights and biases for WSL, Base Shear, and Overturning Moment are shown in the Table.2, Table.3, and Table .4, respectively. To compare actual data with the data generated by the NARX, Figures.16-18 show the set of time series for the water surface level, base shear, and overturning moment, respectively. The time series were predicted using the NARX neural network model and the actual data recorded in the NIMALA marine laboratory (Fig.16-18). Table.2 shows statistical indices such as maximum, minimum, standard deviation, and median for WSL, base shear, and overturning moment (Table.5). These statistical indexes are calculated for actual and

predicted data. A few differences between actual and predicted statistical indexes could be seen, especially for maximum and minimum indexes.

Table 2 - The optimum values of NARX model, used for WSL data estimating

Weight matrix and bias vector for NARX model (wsl)										
$IW_1^{1,1}$	-1.047E+00	1.080E+00	$IW_2^{1,1}$	-1.190E+00	1.486E+00	b^1	2.286E+00	b^2	1.157E+00	
	2.112E+00	6.022E-01		3.724E-01	-1.652E+00		-1.921E+00			
	-1.082E+00	9.068E-01		1.367E+00	-4.364E-01		8.487E-01			
	1.302E+00	1.265E+00		1.326E+00	-9.052E-01		-8.692E-01			
	-3.906E-01	-7.343E-01		-2.053E+00	9.293E-01		1.352E-01			
	-1.661E+00	1.321E+00		1.319E+00	-8.374E-01		-5.872E-01			
	-1.605E+00	1.615E+00		4.443E-01	1.169E-01		-3.291E-01			
	4.921E-01	-5.749E-01		-1.081E+00	1.026E+00		6.438E-01			
	-4.229E-01	3.471E-01		-1.493E+00	1.920E+00		-1.949E+00			
	-2.652E-02	-1.244E+00		-1.631E+00	-9.314E-02		-2.138E+00			
$LW^{2,1}$	-6.784E-01	7.111E-04	4.148E-01	-3.209E-03	-5.361E-02	2.931E-01	1.161E+00	-8.242E-01	-1.541E-01	-7.100E-02

Table 3 - The optimum values of NARX model, used for base shear data estimating

Weight matrix and bias vector for NARX model (Base Shear)											
$IW_1^{1,1}$	-1.549E+00	8.186E+00	3.280E-01	2.927E+00	$IW_2^{1,1}$	1.699E+00	8.474E+00	b^1	5.696E+00	b^2	-3.995E-01
	1.138E+00	-1.775E+00	-7.248E-01	6.965E-01		2.637E+00	-1.354E+00		9.223E-01		
	-6.041E-02	-6.632E-02	4.754E-02	1.733E-02		2.764E+00	-2.517E+00		-1.813E-01		
	-7.014E-01	-7.240E+00	9.769E-01	2.632E+00		3.397E+00	3.156E-01		1.515E+00		
	-5.892E+00	-5.223E+00	-4.504E+00	-6.164E-01		5.589E+00	-1.494E+00		2.005E+00		
	-1.437E+00	2.098E-01	-1.852E+00	2.095E+00		-7.683E-01	1.839E+00		5.381E-01		
	4.280E-01	2.472E-01	-4.350E-01	-2.322E-01		3.994E-01	-9.338E-01		1.011E-02		
	-9.433E-02	-2.037E+00	-3.555E-01	-1.572E+00		1.820E+00	-2.364E+00		-2.603E-01		
	8.436E-01	7.711E-01	-9.087E-01	-5.764E-01		1.374E+00	-1.057E+00		7.921E-01		
	-1.571E+00	6.378E-01	-1.947E+00	-9.787E-01		-4.216E+00	3.090E+00		-2.796E+00		
$LW^{2,1}$	-5.899E-03	4.233E-02	4.157E-01	-1.073E-02		-4.983E-03	-7.419E-03	-1.411E+00	3.199E-02	7.093E-01	-9.485E-03

Table 4 - The optimum values of NARX model, used for overturning moment data estimating

Weight matrix and bias vector for NARX model (Overturning Moment)											
$IW_1^{1,1}$	-9.682E-01	-1.100E+00	1.060E+00	-1.745E-01	$IW_2^{1,1}$	-1.007E+00	4.797E-01	b^1	1.844E+00	b^2	-2.620E-01
	-9.682E-01	-7.255E-01	1.734E-01	3.069E-01		8.037E-01	-1.154E+00		-1.274E+00		
	-2.790E-01	2.312E-01	2.901E-01	2.464E-02		-1.724E+00	1.706E-02		-4.371E-01		
	-4.692E-01	-1.643E-01	-8.163E-01	6.281E-01		7.480E-01	-8.429E-01		1.206E+00		
	-7.251E-03	-7.063E-01	-1.939E-01	6.705E-01		-1.590E+00	2.689E-01		-5.508E-01		
	-7.829E-01	-7.428E-01	2.667E-01	1.371E+00		-5.367E-01	1.001E+00		-3.156E-01		
	8.014E-01	4.096E-02	-4.932E-01	-1.057E+00		-1.720E+00	-1.321E+00		4.893E-01		
	2.753E-01	3.072E-01	-6.179E-01	-7.359E-01		-1.373E+00	-1.305E+00		1.188E+00		
	6.899E-01	-1.243E+00	-9.560E-01	1.558E+00		-1.862E+00	4.647E-01		9.296E-01		
	9.511E-01	2.384E-01	-8.780E-01	-5.630E-01		-1.490E+00	6.730E-01		7.725E-01		
$LW^{2,1}$	6.964E-01	8.063E-02	-1.228E-01	1.467E-01	-3.320E-01	1.806E-01	6.680E-02	-9.652E-02	-3.100E-01	-5.045E-01	

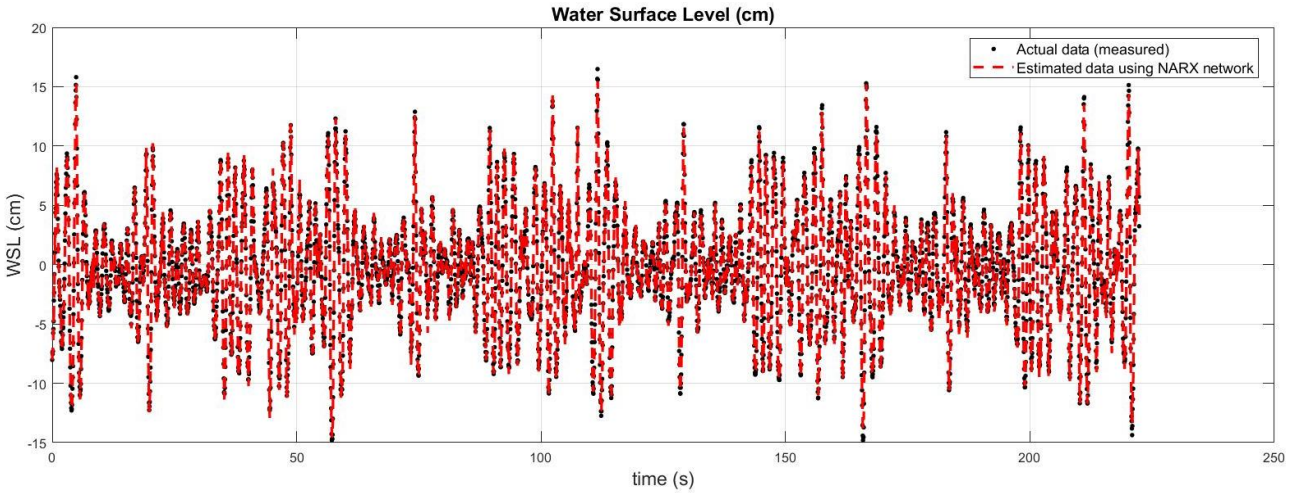

Fig. 16 - Time series of recorded WSL and predicted WSL using NARX model

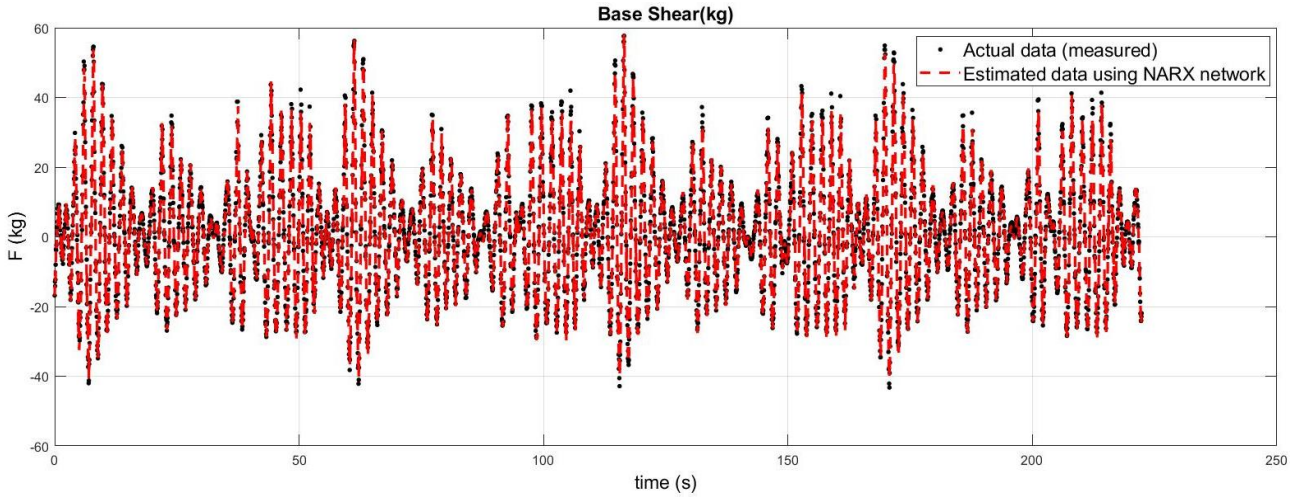

Fig. 17 - Time series of recorded base shear and predicted base shear using NARX model

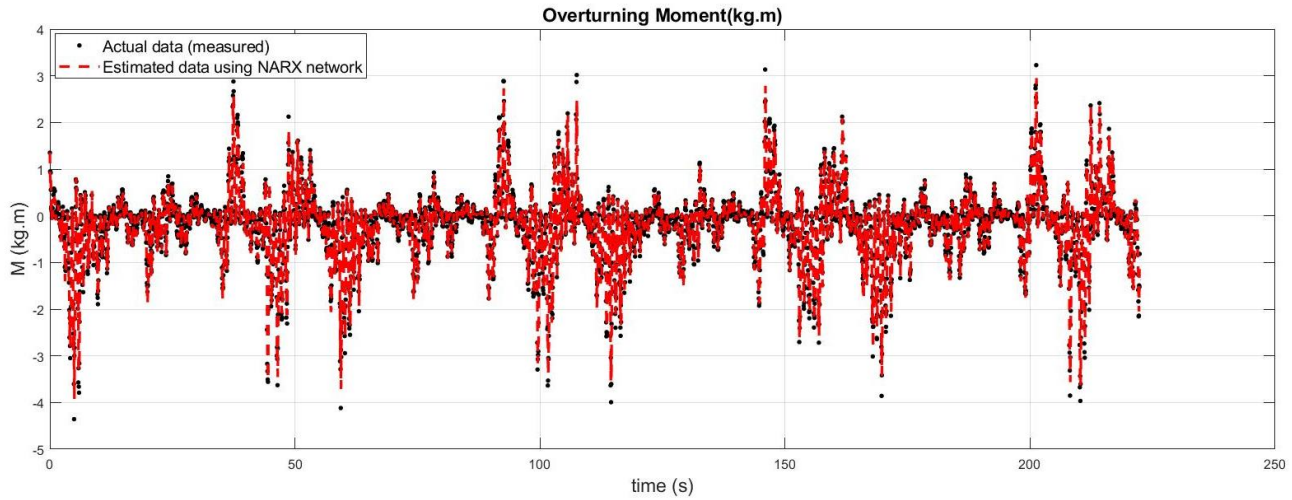

Fig. 18 - Time series of recorded overturning moment and predicted overturning moment using NARX model

Table 5 - The optimum values of NARX model, used for overturning moment data estimating

	Actual data (measured)				Produced data with NARX			
	min	max	std	median	min	max	std	median
WSL	-14.8107	16.4846	4.8860	-0.4193	-14.6778	15.2319	4.7846	-0.1584
F	-43.2472	57.6897	16.5770	0.6694	-43.2556	55.6668	16.1763	0.6698
M	-4.0505	3.44194	0.79407	-0.0568	-3.6364	3.0021	0.7419	-0.0589

5. Conclusion

An artificial neural network (ANN) is a data-driven mathematical model that has been developed to imitate the structure of the neural network of a human brain and has been widely applied to solve problems such as prediction and discrimination (Lee et al., 2018). The ANN method is used extensively in many scientific and technological fields, such as predicting the future values of time series. The current study investigated the possibility of predicting base shear and the overturning moment based on the time and water surface level data as input data using the NARX neural network.

In the present research, a jacket model with a height of 4.55m was fabricated and tested in the wave flume of the NIMALA marine laboratory. The wave flume was 402m long. The jacket was tested at the water depth of 4m and subjected to JONSWAP waves with the input wave height of 20cm, 23cm, and 28cm. The mechanism of wave energy dissipation due to hitting a wave barrier was mainly a combination of wave diffraction and wave reflection.

As shown in Fig 10 and Fig 11, the final correlation values (R) for water surface level (WSL) estimated with NAR and NARX networks are 0.028 and 0.994, respectively. As a result, due to the inappropriateness of the correlation value for NAR, this network cannot be used to estimate WSL values, probably because the time component is not included in the NAR network. In the next step, the obtained correlation value for Base Shear and Overturning Moment time-series estimated using the NARX network and considering time and WSL as input values were 0.97 and 0.94, respectively. It can be concluded that base shear and overturning moment can be estimated by time and WSL using the NARX network.

However, it should be noted that the results were obtained according to precise measurements in the NIMALA laboratory. Thus, the performance of the ANN method is likely to be different in natural coastal environments, and it is necessary to investigate the issue in practical conditions. As a hybrid method, the Adaptive Neuro-Fuzzy Inference System (ANFIS) can help investigate the structure behaviour against random waves with and without wave barriers. Hopefully, it will turn into a field of discussion for future researchers.

Abbreviations

NIMALA	National Iranian Marine Laboratory	HSC	High-Strength Concrete
NARX	Nonlinear Autoregressive Exogenous Neural Network	AI	Artificial Intelligence
ANN	Artificial Neural Network	WSL	Water Surface Level
NAR	Nonlinear Autoregressive Neural Network	JONSWAP	Joint North Sea Wave Project
RNN	Recurrent Neural Network	P-M	Pierson-Moskowitz
CHS	Circular Hollow Section	LMA	Levenberg-Marquardt Algorithm
HW	Holt-Winters	ARIMAX	Autoregressive Integrated Moving Average with Explanatory

References

Afroz, Z., Urmee, T., Shafiullah, G., & Higgins, G. (2018). Real-time prediction model for indoor temperature in a commercial building. *Applied energy*, 231, pp.29-53.

Aalami, M., Vafaeipoor, R., Naseri, A., Mojtahedi, A. (2022). Experimental Analysis of the Effect of the Distance of a Submerged Berm in front of a Reshaping Rubble Mound Breakwater on Diminishing the Damage Parameter. *Journal of Civil and Environmental Engineering*, 52.2(107), pp.1-13. doi: 10.22034/jcee.2021.45699.2028

Alami, M. T., Vafaeipour Sorkhabi, R., Naseri, A., & Mojtahedi, A. (2022). Enhancing Stability and Reduce Damage in Rubble-Mound Reshaping Breakwaters by Using Obstacles in Front of the Structure. *Civil Infrastructure Researches*, 7(2), pp.33-49. doi: 10.22091/cer.2021.7367.1297

Amin, J. S., Bahadori, A., Mohamadi, E., & Nia, B. H. (2015). Predicting natural gas hydrate formation temperature using Levenberg-Marquardt algorithm. *Petroleum Science and Technology*, 33(9), pp.1038-1044.

Arif, J., Chaudhuri, N. R., Ray, S., & Chaudhuri, B. (2009). Online Levenberg-Marquardt algorithm for neural network based estimation and control of power systems. *2009 International Joint Conference on Neural Networks.*

Blanchard, T., & Samanta, B. (2020). Wind speed forecasting using neural networks. *Wind Engineering,* 44(1), PP.33-48.

Boussaada, Z., Curea, O., Remaci, A., Camblong, H., & Mrabet Bellaaj, N. (2018). A nonlinear autoregressive exogenous (NARX) neural network model for the prediction of the daily direct solar radiation. *Energies,* 11(3), 620.

Chan, E.-S., Cheong, H.-F., & Tan, B.-C. (1995). Laboratory study of plunging wave impacts on vertical cylinders. *Coastal Engineering,* 25(1-2), pp.87-107.

Diaconescu, E. (2008). The use of NARX neural networks to predict chaotic time series. *Wseas Transactions on computer research,* 3(3), pp.182-191.

Do Nascimento Camelo, H., Lucio, P. S., Junior, J. B. V. L., de Carvalho, P. C. M., & dos Santos, D. v. G. (2018). Innovative hybrid models for forecasting time series applied in wind generation based on the combination of time series models with artificial neural networks. *Energy,* 151, pp.347-357.

Esandi, J. M., Buldakov, E., Simons, R., & Stagonas, D. (2020). An experimental study on wave forces on a vertical cylinder due to spilling breaking and near-breaking wave groups. *Coastal Engineering,* 162, 103778.

Goda, Y., Haranaka, S., & Kitahara, M. (1966). *Study of Impulsive Breaking Wave Forces on Piles (in Japanese).* Report of Port and Harbour Research Institute Ministry of Transport, Japan, 5(6).

Guo, J., Wu, J., Guo, J., & Jiang, Z. (2018). A damage identification approach for offshore jacket platforms using partial modal results and artificial neural networks. *Applied Sciences,* 8(11), 2173.

Hildebrandt, A. (2013). *Hydrodynamics of breaking waves on offshore wind turbine structures,* Hannover: Gottfried Wilhelm Leibniz Universität Hannover.

Lee, J., Kim, C.-G., Lee, J. E., Kim, N. W., & Kim, H. (2018). Application of artificial neural networks to rainfall forecasting in the Geum River basin, Korea. *Water,* 10(10), 1448.

Li, W., & Huang, Y. (2020). A combined method of cross-correlation and PCA-based outlier algorithm for detecting structural damages on a jacket oil platform under random wave excitations. *Applied Ocean Research,* 102, 102301.

Morison, J., Johnson, J., & Schaaf, S. (1950). The force exerted by surface waves on piles. *Journal of Petroleum Technology,* 2(05), pp.149-154.

Mousavi, Z., Varahram, S., Ettefagh, M. M., Sadeghi, M. H., & Razavi, S. N. (2021). Deep neural networks–based damage detection using vibration signals of finite element model and real intact state: An evaluation via a lab-scale offshore jacket structure. *Structural Health Monitoring,* 20(1), pp.379-405.

Naseri, A., Vafaeipour Sorkhabi, R., Alami, M. T., & Mojtahedi, A. (2022). Damage Parameter Variations of Breakwater along with a Floating Wave Barrier and a Submerged Obstacle. *International Journal of Sustainable Construction Engineering and Technology,* 13(1), pp.202–217.

Osgouei, A. D., Poursorkhabi, R. V., Maleki, A., & Ahmadi, H. (2021). Effects of a floating wave barrier with square cross section on the wave-induced forces exerted to an offshore jacket structure. *Ocean Systems Engineering,* 11(3), pp.259-274.

Raptodimos, Y., & Lazakis, I. (2020). Application of NARX neural network for predicting marine engine performance parameters. *Ships and Offshore Structures,* 15(4), pp.443-452.

Sarkar, R., Julai, S., Hossain, S., Chong, W. T., & Rahman, M. (2019). A comparative study of activation functions of NAR and NARX neural network for long-term wind speed forecasting in Malaysia. *Mathematical Problems in Engineering,* 2019.

Shahrisvand, M., Akhoondzadeh, M., & Sharifi, M. A. (2014). Detection of gravity changes before powerful earthquakes in GRACE satellite observations. *Annals of Geophysics,* 57(5), 0543.

Shariati, M., Mafipour, M. S., Mehrabi, P., Bahadori, A., Zandi, Y., Salih, M. N., Nguyen, H., Dou, J., Song, X., & Poi-Ngian, S. (2019). Application of a hybrid artificial neural network-particle swarm optimization (ANN-PSO) model in behavior prediction of channel shear connectors embedded in normal and high-strength concrete. *Applied Sciences,* 9(24), 5534.

Shariati, M., Mafipour, M. S., Mehrabi, P., Shariati, A., Toghroli, A., Trung, N. T., & Salih, M. N. (2020). A novel approach to predict shear strength of tilted angle connectors using artificial intelligence techniques. *Engineering with Computers,* pp.1-21.

Sruthi, C., & Sriram, V. (2017). Wave impact load on jacket structure in intermediate water depth. *Ocean Engineering,* 140, 183-194.

Stathakis, D. (2009). How many hidden layers and nodes? *International Journal of Remote Sensing,* 30(8), pp.2133-2147.

Taherdangkoo, R., Tatomir, A., Taherdangkoo, M., Qiu, P., & Sauter, M. (2020). Nonlinear autoregressive neural networks to predict hydraulic fracturing fluid leakage into shallow groundwater. *Water,* 12(3), 841.

Vafaeipour Sorkhabi, R., Naseri, A., Alami, M.T. et al. (2022). Experimental study of an innovative method to reduce the damage of reshaping rubble mound breakwaters. *Innovative Infrastructure Solutions*, 7, 353. doi: 10.1007/s41062-022-00954-1

Vafaeipour Sorkhabi, R., & Naseri, A. (2019). Experimental Investigation of the Interaction between Vertical Flexible Seawall and Random Sea Waves. *Journal of Advanced Defence Science and Technology*, 6(3), pp.155-162.

Vfaeipour sorkhabi, R., Alami, M., Naseri, A., & Mojtahedi, A. (2022). Experimental Analysis of the Effect of a Submerged obstacle and Floating Wave Barrier in front of a Rubble Mound Breakwater on Diminishing the Damage Parameter. *International Journal of Coastal and Offshore Engineering*, 7(2), pp.39-48.

Wei, S., Zuo, D., & Song, J. (2012). Improving prediction accuracy of river discharge time series using a Wavelet-NAR artificial neural network. Journal of Hydroinformatics, 14(4), pp.974-991.

Xiu, Y., & Zhang, W. (2017). Multivariate chaotic time series prediction based on NARX neural networks. *Proc. 2nd Int. Conf. Electr.*, Autom. Mech. Eng.(EAME).

Zounemat-Kermani, M., Stephan, D., & Hinkelmann, R. (2019). Multivariate NARX neural network in prediction gaseous emissions within the influent chamber of wastewater treatment plants. *Atmospheric Pollution Research*, 10(6), pp.1812-1822.